Quantum Electronics **40** (10) 899–906 (2010)

NONLINEAR OPTICAL PHENOMENA

PACS numbers: 42.60.Jf; 42.65.Tg; 42.70.Nq
DOI: 10.1070/QE2010v040n10ABEH014373

Interaction of two-dimensional orthogonally polarised super-Gaussian light beams in a photorefractive crystal

V.V. Davydovskaya, V.V. Shepelevich, V. Matusevich, A. Kiessling, R. Kowarschik

Abstract. **Propagation and interaction of orthogonally polarised two-dimensional super-Gaussian light beams is studied theoretically in a 4mm-symmetry photorefractive crystal in the drift regime when the external electric field is applied to the crystal in the direction of the optical axis. The output beams displaced with respect to each other in directions parallel and perpendicular to the direction of the external electric field strength vector are considered. It is shown that an auxiliary light beam polarised orthogonally to the fundamental light beam makes it possible to carry out efficiently address localisation of the fundamental beam propagating in a quasi-soliton regime. The crystal thicknesses are found, which are optimal from the viewpoint of maximisation of the fundamental light beam deviation. It is shown that 'square' super-Gaussian beams in the near-field diffraction region are focused at smaller values of the external electric field than those of the Gaussian beams.**

Keywords: *photorefractive crystal, orthogonal polarisations, square super-Gaussian beam, Gaussian beam, beam interaction, crystal of the class 4mm, SBN crystal.*

1. Introduction

Studying the interaction of quasi-soliton light beams in nonlinear media is of interest in view of the prospects for designing all-optical switching and localisation devices based on these media. Recently, there have published many papers devoted to investigations of interaction of light beams in photorefractive crystals.

Some papers consider coherent and incoherent interaction of two-dimensional Gaussian light beams with the same linear polarisation in the photorefractive strontium barium niobate (SBN) $Sr_{0.61}Ba_{0.39}Nb_2O_6$ crystal. They show that coherent interaction of the light beams can lead to their mutual attraction and complete fusing as well as to the mutual repulsion (see, for example, [1, 2]).

Khmelnitsky et al. [3] compared the results of the experiment on interaction (in the SBN crystal) of the so-called square and rectangular two-dimensional light beams polarised in parallel to the optical axis of the crystal with the theoretical results.

Shepelevich et al. [4, 5] studied theoretically interaction of orthogonally polarised one-dimensional Gaussian light beams in cubic optically active crystals. They showed that this interaction makes it possible to efficiently control the address localisation of a quasi-soliton linearly polarised light beam by an auxiliary divergent orthogonally polarised beam.

The authors of papers [6, 7] presented the theory of propagation of one-dimensional orthogonally polarised soliton light beams in anisotropic photorefractive crystals. However, they placed the primary emphasis upon searching for mutual positions of the beams with respect to the external electric field where the soliton regime is realised for both beams, while the control of propagation of one beam with the help of the other was considered indirectly.

In some papers (for example, [2, 8]) studying interaction of two-dimensional light beams in uniaxial crystals, expressions for the potential of the internal electric field take into account only the drift component and neglect the diffusion component. In addition, many papers (for example, [1, 2]) consider the beams with the Gaussian intensity distribution.

At the same time, some papers have been recently published (see, for example, [9]), showing that two-dimensional flat-topped light beams (super-Gaussian beams are the specific case of such beams) have some advantage over Gaussian beams. In particular, in the free propagation regime their divergence in the near-field diffraction region is significantly smaller than that of Gaussian beams. Thus, to ensure the quasi-soliton propagation regime with the use of the external electric field is possible by employing the electric field strength weaker than that in Gaussian beams.

Characteristics of generation and application of different light beams, including super-Gaussian beams, were studied in papers [9–11]. Scientific papers usually consider two types of two-dimensional super-Gaussian light beams – cylindrical and square (see, for example, [12]). Square super-Gaussian beams have a larger store of light energy than the Gaussian and cylindrical super-Gaussian beams and require fewer electric fields to focus in the near-field diffraction region.

In this paper we present the results of theoretical investigations of two-dimensional orthogonally polarised square super-Gaussian beams in the SBN crystal, taking into account the diffusion and drift mechanisms of photorefraction, and compare their interaction with that of Gaussian beams under the same conditions.

2. Theory

Consider incoherent interaction of two monochromatic light beams normally incident on the face of the 4mm-symmetry photorefractive crystal whose optical axis lies in the face plane

V.V. Davydovskaya, V.V. Shepelevich I.P. Shamyakin Mozyr State Pedagogical University; ul. Studencheskaya 28, 247760 Mozyr, Belarus; e-mail: davalenta@inbox.ru, vasshep@inbox.ru;
V. Matusevich, A. Kiessling, R. Kowarschik Friedrich-Schiller-Universität Jena, Germany, D-07743 Jena, Fröbelstieg, 1;
e-mail: Richard.kowarschik@uni-jena.de, oik@uni-jena.de, vladislav.matusevich@uni-jena.de

Received 7 June 2010; revision received 16 September 2010
Kvantovaya Elektronika **40** (10) 899–906 (2010)
Translated by I.A. Ulitkin

while the other crystallographic axis is directed inside the crystal along the normal to this face.

If we assume that the natural crystal anisotropy markedly exceeds the additional change in the dielectric constant induced by the external electric field, this change can be interpreted as perturbation and ordinary and extraordinary waves in the crystal can be treated as unperturbed modes of the beam's light field.

We will direct the x axis of the working coordinate system along the crystallographic axis $\boldsymbol{c}$, which is the optical axis of the crystal. Let the external electric field E_0 be also directed parallel to the optical axis $\boldsymbol{c}$. The z axis is directed along the crystallographic axis $\boldsymbol{a}$, while the y axis – along the crystallographic axis $\boldsymbol{b}$. Then, Maxwell's equations and basic equations of the photorefractive effect [13] make it possible to derive, using the covariant representation [14] of the electro-optic tensor of the 4mm-class crystal, the system of equations in the paraxial approximation, which describes a change in the vector envelope projections of the electric field strengths of the first (A_1) and second (A_2) light beams on the axis x and y:

$$\mathrm{i}\frac{\partial A_{1y}}{\partial z}+\frac{1}{2k_0n_\mathrm{o}}\left(\frac{\partial^2A_{1y}}{\partial x^2}+\frac{\partial^2A_{1y}}{\partial y^2}\right)-\frac{k_0n_\mathrm{o}^3}{2}A_{1y}r_{13}\left(E_0-\frac{\partial\varphi}{\partial x}\right)=0,$$

$$\mathrm{i}\frac{\partial A_{1x}}{\partial z}+\frac{1}{2k_0n_\mathrm{e}}\left(\frac{\partial^2A_{1x}}{\partial x^2}+\frac{\partial^2A_{1x}}{\partial y^2}\right)+\frac{k_0n_\mathrm{e}^3}{2}A_{1x}r_{42}\frac{\partial\varphi}{\partial y}=0,$$

$$\mathrm{i}\frac{\partial A_{2x}}{\partial z}+\frac{1}{2k_0n_\mathrm{e}}\left(\frac{\partial^2A_{2x}}{\partial x^2}+\frac{\partial^2A_{2x}}{\partial y^2}\right)-\frac{k_0n_\mathrm{e}^3}{2}A_{2x}r_{33}\left(E_0-\frac{\partial\varphi}{\partial x}\right)=0, \quad (1)$$

$$\mathrm{i}\frac{\partial A_{2y}}{\partial z}+\frac{1}{2k_0n_\mathrm{o}}\left(\frac{\partial^2A_{2y}}{\partial x^2}+\frac{\partial^2A_{2y}}{\partial y^2}\right)+\frac{k_0n_\mathrm{o}^3}{2}A_{2y}r_{42}\frac{\partial\varphi}{\partial x}=0.$$

Here, k_0 is the modulus of the wave vector of the light beams in vacuum; n_o and n_e are the refractive indices of ordinary and extraordinary waves; E_0 is the projection of the $\boldsymbol{E}_0$ vector on the x axis; r_{13}, r_{33}, and r_{43} are the electro-optic tensor components of the crystal; φ is the found electric potential related to the spatial charge field potential ϕ by the expression

$$\varphi=\phi+E_0x \quad (2)$$

and determined from the equation (see, for example, [15, 16])

$$\nabla^2\varphi+\nabla\ln(1+I)\nabla\varphi-\frac{k_\mathrm{B}T}{q}\{\nabla^2\ln(1+I)+[\nabla\ln(1+I)^2]\}$$

$$=E_0\frac{\partial}{\partial x}\ln(1+I), \quad (3)$$

where

$$I=\frac{n_\mathrm{o}\left(|A_{1x}|^2+|A_{2x}|^2\right)+n_\mathrm{e}\left(|A_{1y}|^2+|A_{2y}|^2\right)}{2\eta_0I_\mathrm{d}} \quad (4)$$

is the relative light field intensity in the region of incoherent interaction of light beams; I_d is the dark intensity including the background noise; k_B is the Boltzmann constant; T is the absolute temperature; q is the elementary charge; $\eta_0=\sqrt{\mu_0/\varepsilon_0}$ [17]. Note that in studying coherent interaction of the light beams or in determining polarisation of the light transmitted through the crystal, we should take into account different phase shift of ordinary and extraordinary waves at a fixed coordinate z. The term in the left-hand side of equation (3), containing the multiplier $k_\mathrm{B}T/q$, corresponds to the electron diffusion in a photorefractive crystal (diffuse term). The expression in the right-hand side of (3) containing E_0 is responsible for the electron drift in the external electric field. Thus, the regime of propagation and interaction of the light beams at $E_0\neq0$ is called the drift regime.

We assume that the first beam at the crystal input is linearly polarised, perpendicular to the external electric field vector $\boldsymbol{E}_0$ (ordinary wave), while the second beam is linearly polarised, parallel to the vector $\boldsymbol{E}_0$ (extraordinary wave), i.e.,

$$A_{1y}\big|_{z=0}=A_{01},\quad A_{1x}\big|_{z=0}=0,$$

$$A_{2x}\big|_{z=0}=A_{02},\quad A_{2y}\big|_{z=0}=0. \quad (5)$$

Numerical estimates show that when conditions (5) are met at the SBN crystal output under typical conditions, the inequalities $|A_{1x}|^2\ll|A_{1y}|^2$, $|A_{2y}|^2\ll|A_{2x}|^2$ are fulfilled and the contribution of the components A_{1x} and A_{2y}, which become nonzero in calculations, can be neglected in the resultant intensity (4) calculated at each step and determining the relation between the orthogonal components of the beams. Thus, the system of equations (1) can be approximately replaced by a system of two differential equations in partial derivatives:

$$\mathrm{i}\frac{\partial A_{1y}}{\partial z}+\frac{1}{2k_0n_\mathrm{o}}\left(\frac{\partial^2A_{1y}}{\partial x^2}+\frac{\partial^2A_{1y}}{\partial y^2}\right)-\frac{k_0n_\mathrm{o}^3}{2}A_{1y}r_{13}\left(E_0-\frac{\partial\varphi}{\partial x}\right)=0,$$

$$\mathrm{i}\frac{\partial A_{2x}}{\partial z}+\frac{1}{2k_0n_\mathrm{e}}\left(\frac{\partial^2A_{2x}}{\partial x^2}+\frac{\partial^2A_{2x}}{\partial y^2}\right)-\frac{k_0n_\mathrm{e}^3}{2}A_{2x}r_{33}\left(E_0-\frac{\partial\varphi}{\partial x}\right)=0. \quad (6)$$

3. Numerical simulation of interaction of two-dimensional light beams with super-Gaussian and Gaussian intensity distributions in a photorefractive SBN crystal

Simulating interaction of two-dimensional light beams in the SBN crystal, we used the parameters: $n_\mathrm{o}=2.36$; $n_\mathrm{e}=2.33$; $\lambda=0.5145$ μm; $r_{13}=47$ pm V^{-1}; $r_{33}=235$ pm V^{-1} (see, for example, [18, 19]); $E_0=0.8$ kV cm^{-1}; the crystal length, 30 mm; the

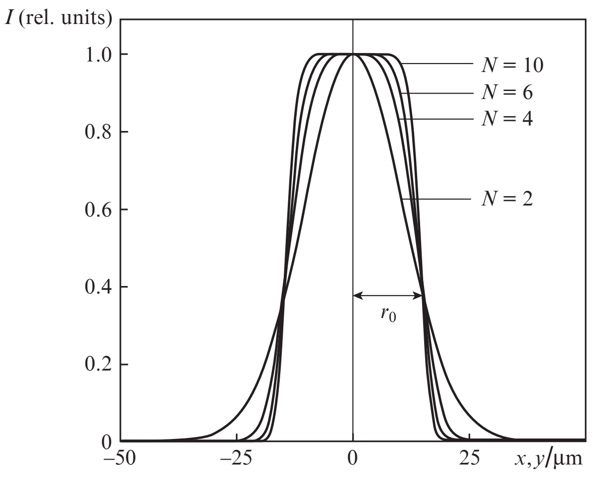

Figure 1. Profiles of different-order super-Gaussian-beam cross sections.

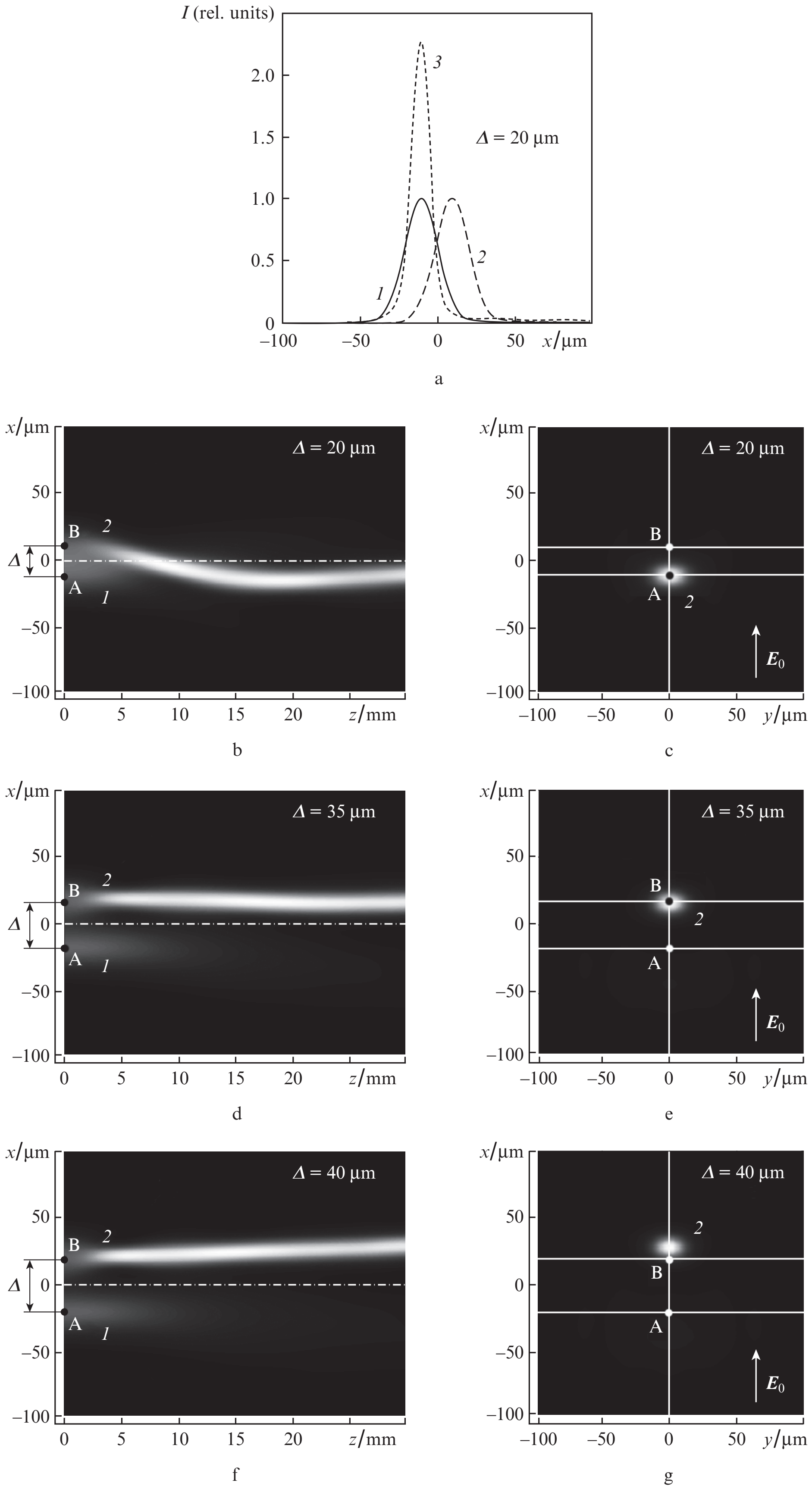

Figure 2. Calculation results of interaction of Gaussian light beams with the centres displaced by a distance Δ parallel to the external electric field vector, by neglecting electron diffusion in the crystal: cross sections of Gaussian beams at the crystal input (*1*, *2*) and the resultant beam at the crystal output (*3*) by a plane parallel to the plane xz and passing through the point at which the intensity maximum is achieved (a); light field distribution over the crystal thickness (b, d, f); position of the quasi-soliton beam (*2*) at the crystal output (c, e, g).

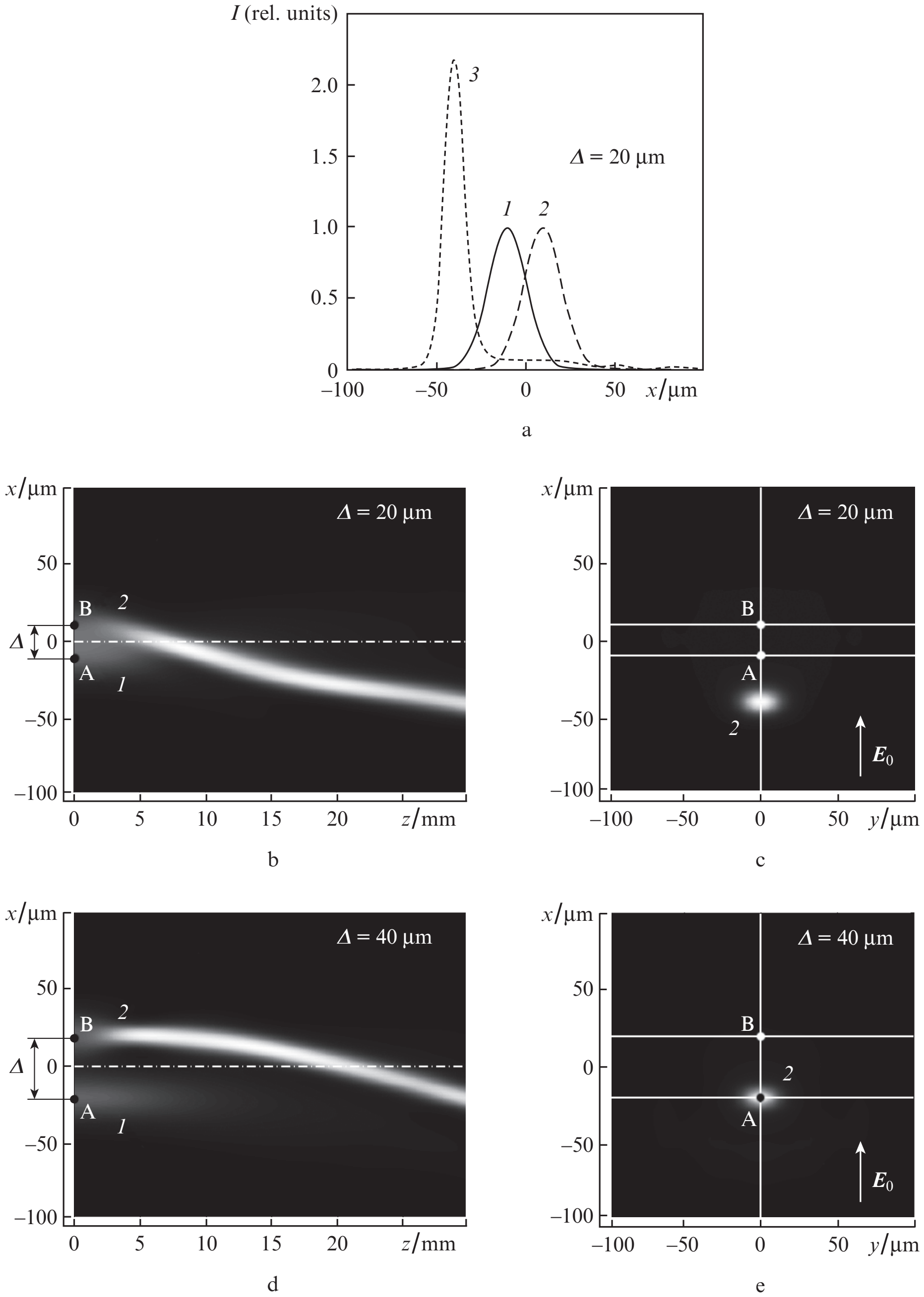

Figure 3. Calculation results of interaction of Gaussian light beams with the centres displaced by a distance Δ parallel to the external electric field vector, with allowance for electron diffusion in the crystal: cross sections of Gaussian beams at the crystal input (*1*, *2*) and the resultant beam at the crystal output (*3*) by a plane parallel to the plane xz and passing through the point at which the intensity maximum is achieved (a); light field distribution over the crystal thickness (b, d); position of the quasi-soliton beam (*2*) at the crystal output (c, e).

characteristic cross sections of the output beams, $r_0 = 15$ μm; the distance between the beam centres, $\Delta = 20$ μm. The optical axis of the crystal is directed along the x axis.

The relative intensity I of the square super-Gaussian beam at the crystal input is described by the expression (see, for example, [12, 20–22])

$$I = \frac{I_0}{I_\mathrm{d}} \exp\left[\frac{-(x^N + y^N)}{r_0^N}\right], \quad (7)$$

where N is the super-Gaussian beam order. Note that at $N = 2$, expression (7) describes a Gaussian beam. In this case, r_0 is called the beam radius. We assume below that $I_0 = I_\mathrm{d}$, i.e., the maximal relative intensity of the light beams (7) is equal to unity at the crystal input (Fig. 1).

Let us analyse first the interaction of orthogonally polarised Gaussian ($N = 2$) light beams [curves (*1*) and (*2*) in Fig. 2a] displaced with respect to each other by $\Delta = 20$ μm along the direction of the external electric field strength vector $\boldsymbol{E}_0$, by neglecting the diffusion term in the equation for the potential. Beam (*1*) is polarised perpendicular to the external electric field strength vector, while beam (*2*) – parallel to this vector. Point A in Fig. 2 indicates the initial position of the centre of beam (*1*) at the crystal input, while point B shows the initial position of the centre of beam (*2*). The horizontal dashed line (Figs 2b, d, f) and intersecting solid lines (Figs 2c, e, g) are

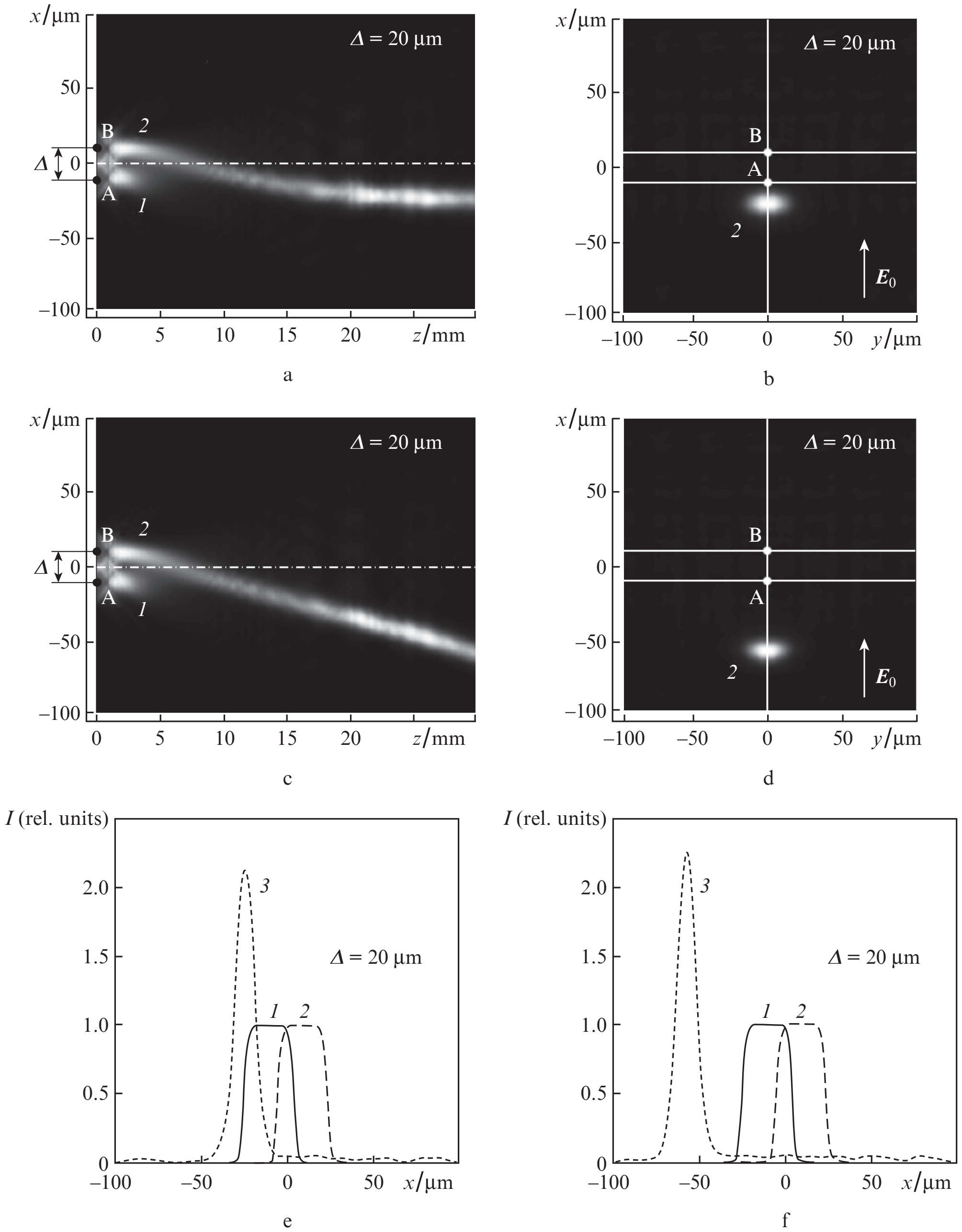

Figure 4. Calculation results of interaction of super-Gaussian light beams with the centres displaced by a distance Δ parallel to the external electric field vector: light field distribution over the crystal thickness without (a) and with (c) the electron diffusion; position of the quasi-soliton beam (*2*) at the crystal output without (b) and with (d) the diffusion; cross sections of the beams by a plane parallel to the plane xz and passing through the point at which the intensity maximum is achieved without (e) and with (f) the diffusion [cross sections of super-Gaussian beams at the crystal input (*1*, *2*) and cross section of the resultant beam at the crystal output (*3*)].

shown for convenient comparison of the beam positions at the crystal input and output.

If we neglect the intensity of the output beam (*1*), which is virtually scattered and can be called auxiliary, beam (*2*) can be treated as a resultant beam. Because the interacting beams are attracted, the quasi-soliton beam (*2*) deviates and occupies (at the crystal output) the position of beam (*1*) (Fig. 2c), which is strongly scattered, but nevertheless plays the role of the control beam (Fig. 2b). Without beam (*1*) and electron diffusion in the crystal, beam (*2*) does not deviate. As the distance between the beam centres increases up to 35 μm, the beam attraction becomes weaker and the position of beam (*2*) at the crystal output changes insignificantly (Figs 2d, e) compared to the initial position. A further increase in Δ (Δ = 40 μm, Figs 2f, g) leads to a weak repulsion of the beams, while at Δ > 100 μm beam (*1*) virtually stops affecting beam (*2*).

Mutual attraction and repulsion of the light beams in their incoherent interaction versus the distance between them was also studied in [23] for the identical linearly polarised beams. If the equation takes into account terms responsible for the electron diffusion in the crystal, we can observe at Δ = 20 μm an additional beam displacement along the x axis in the direction opposite to that of the external electric field strength vector due to the beam self-deflection appearing when diffusion is taken into account. The displacement direction of beam (*2*) during the beam interaction (Figs 2b, c) coincides with the dis-

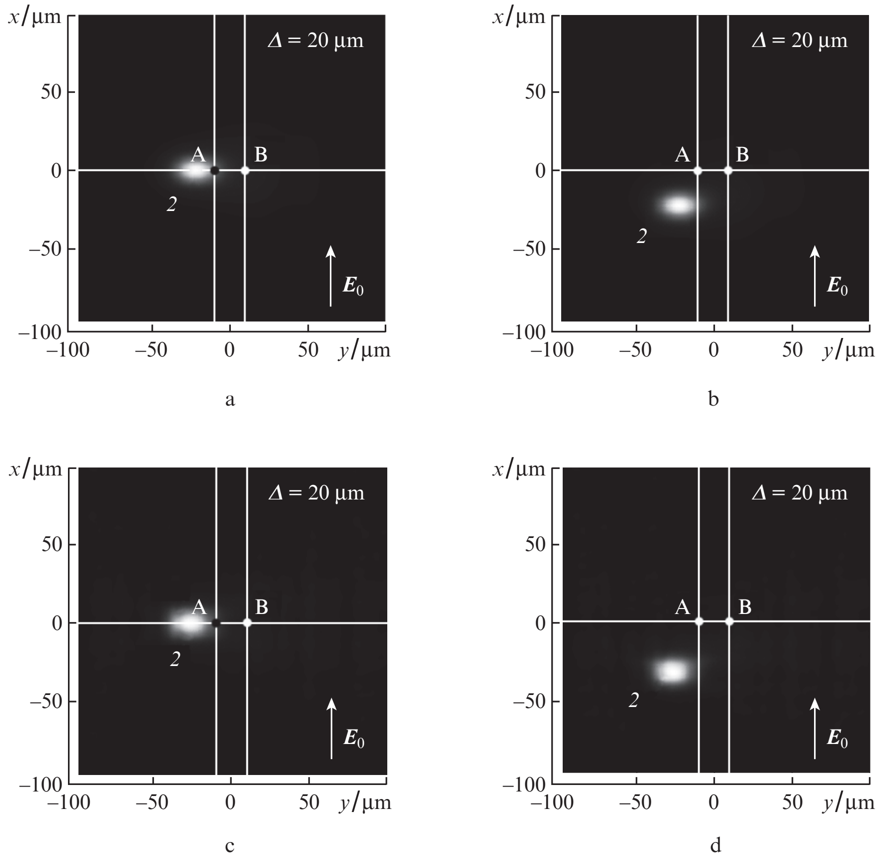

Figure 5. Calculation results of interaction of light beams displaced with respect to each other in the direction perpendicular to the external electric field vector: for Gaussian beams – position of the quasi-soliton beam (*2*) at the crystal output without (a) and with (b) the electron diffusion; for super-Gaussian beams – position of the quasi-soliton beam (*2*) at the crystal output without (c) and with (d) the diffusion.

placement direction of this beam due to self-deflection; therefore, the displacement of the quasi-soliton beam (*2*) in the direction of beam (*1*) increases (Figs 3a, b, c) compared to the displacement shown in Fig. 2. At $\Delta = 40$ μm when the beams repulse due to their interaction (Figs 2f, g), the directions of the above-described displacements are opposite; therefore, the displacement of beam (*2*) along the x axis, caused by the beam interaction, is compensated for by the displacement resulting from the beam self-deflection and the beam repulsion is virtually absent (Figs 3d, e). Figure 4 presents the results of calculation of the interacting square super-Gaussian ($N = 10$) orthogonally polarised light beams displaced with respect to each other along the direction of the external electric field strength vector $\boldsymbol{E}_0$ ($\Delta = 20$ μm).

Processes of the self-deflection (due to diffusion) and displacement (due to interaction) of the beams are also observed when they displace with respect to each other in the direction perpendicular to that of the external electric field strength vector. However, in this case the beams self-deflect along the x axis in the direction opposite to that of the external electric field strength vector, while the beam deflection due to their interaction occurs along the y axis in the direction of beam (*1*), and as these effects overlap, beam (*2*) displaces across the x axis (Fig. 5).

One can see from Figs 2–5 that Gaussian and super-Gaussian beams with the above parameters behave similarly. But at the same time, they exhibit a number of distinctions. For example, when we consider interaction of Gaussian light beams without the electron diffusion in the crystal, the optimal crystal length z for the selected parameters (Fig. 2b) is equal to 15 mm because at $z > 15$ mm the deflection of beam (*2*) in the direction of beam (*2*) almost stops; for the super-Gaussian beams (Fig. 4) the optimal value is $z = 25$ mm. We can also point out that the super-Gaussian light beam (*2*) displaces more under the action of beam (*1*) (Figs 5c, d) than the Gaussian beam (Figs 5a, b).

The light beams with the intensity profiles close to the rectangular one (in our case – super-Gaussian) can be conveniently used at a small thickness of the crystal because at the initial stages of transmission through the crystal the profiles of these beams become markedly deformed, which may lead to a significant increase in the beam intensity, i.e., to additional focusing that is not typical of the Gaussian beams. However, the use of the super-Gaussian beams can cause some problems: already at $N > 5$ we observe an increase in the number of 'pulsations' at the edges of the beam profile, which introduces additional errors in calculations [24].

We have found that when in the absence of the external electric field beam (*2*) propagates through a 10-mm-thick crystal and beam (*1*) does not affect it, we observe a monotonic decrease in the maximal relative intensity in the case of a Gaussian beam, while in the case of a super-Gaussian beam there appears an additional self-focusing, which achieves a maximum at $z = 1.8$ mm. This additional self-focusing of square super-Gaussian light beams, taking place in the region $0 < z < 4$ mm, affects their interaction result. We will study this effect by considering interaction of orthogonally polarised Gaussian and super-Gaussian light beams with predetermined

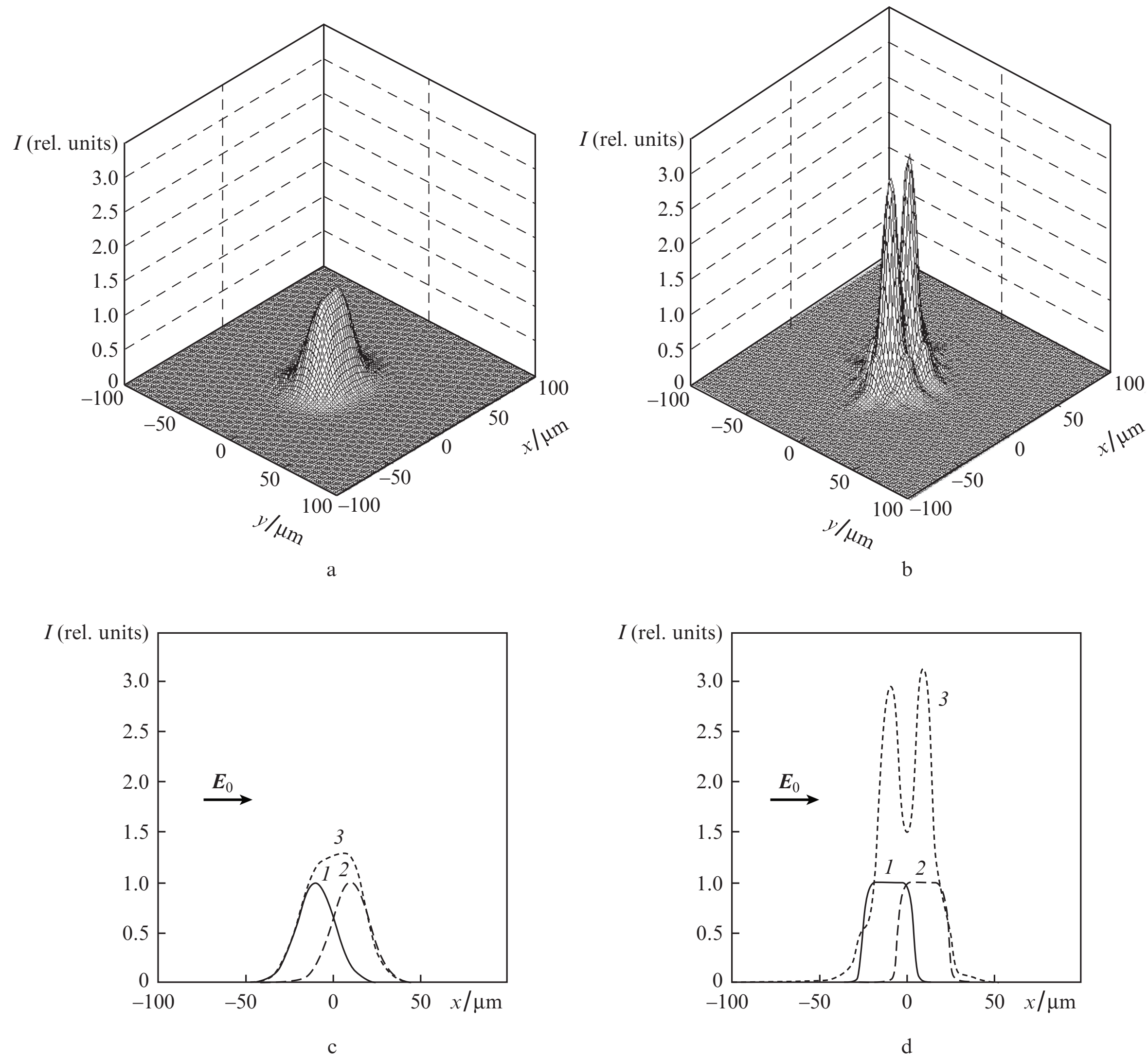

Figure 6. Calculation results of interaction of orthogonally polarised Gaussian and super-Gaussian displaced with respect to each other in the direction parallel to the external electric field vector, by neglecting the electron diffusion in the crystal: Gaussian beams at the crystal output (a); super-Gaussian beams at the crystal output (b); cross sections of Gaussian beams at the crystal output (*1*, *2*) and of the merged beam at the crystal output (*3*) by a plane parallel to the plane xz and passing through the point at which the intensity maximum is achieved (c); cross sections of super-Gaussian beams at the crystal output (*1*, *2*) and of the merged beam at the crystal output (*3*) by a plane parallel to the plane xz and passing through the point at which the intensity maximum is achieved (d).

parameters and $\Delta = 20$ μm in the drift regime without electron diffusion in the crystal. The external electric field E_0 is assumed equal to 0.8 kV cm^{-1}, and the coordinate inside the crystal – to 1.8 mm because at this value of z we observe the maximal additional self-focusing of a solitary super-Gaussian beam propagating in the crystal.

Interaction of Gaussian beams resulted in their fusing at $z = 1.8$ mm (Figs 6a, c). In the case of super-Gaussian beams, we failed to observe their complete fusing, while the beam intensity increased by 3–3.5 times and each beam continued focusing independently.

After the Gaussian light beams interacted, the merged beam becomes asymmetric [Fig. 6c, curve (*3*)] – the right-hand side of the envelope being steeper than the left-hand one. Because the conditions for the diffracted beams are closer to the total internal reflection on the right than on the left, the propagating beam deflects to the left along the x axis if we look at the face of the beam (Fig. 2c) or to the right we look at its tail (Fig. 2b).

The same situation takes place when square super-Gaussian beams interact [one can see from Fig. 6d that the maximal intensity of the right beam is greater than that of the left one, while the right-hand part of the envelope of the total intensity distribution along the x axis is steeper than the left-hand part, which determines a more significant deflection of the beams due to their interaction (Fig. 4c) than in the case of the Gaussian beams (Fig. 3c)].

Recall that bright spatial solitons propagate in a nonlinear medium without diffraction under condition that the refractive index in the beam region is greater than in the adjacent regions. The resultant beam self-focusing compensating for the beam diffraction is also explained by the total internal reflection of the light beams during their diffraction.

4. Conclusions

We have studied the peculiarities of propagation and interaction of orthogonally polarised Gaussian and square super-

Gaussian light beams in a photorefractive SBN crystal placed in the external electric field.

We have shown that during interaction of such orthogonally polarised beams one of the beams retains its quasi-soliton character and experiences deflection under the action of the other beam, which strongly scatters but plays the role of the control one.

We have found that allowance for the diffuse term in the equation for the potential leads to an additional displacement of the light beams along the x axis in the direction opposite to the direction of the external electric field.

We have found the optimal crystal thicknesses for which the deflection of the quasi-soliton light beam during the interaction of two-dimensional orthogonally polarised light beams will be greatest.

We have established differences in propagation and interaction of Gaussian and super-Gaussian two-dimensional light beams. We have found that square super-Gaussian beams require fewer electric fields for focusing in the near-field diffraction region than Gaussian and cylindrical super-Gaussian beams, while cylindrical super-Gaussian beams require fewer electric fields for focusing in the near-field diffraction region than Gaussian beams. A disadvantage of super-Gaussian beams at $N > 5$ is their spatial instability in the far-field diffraction region.

The obtained results can be used to control the beam self-focusing and are of interest for fabricating devices for address switching of the beam positions. They can also stimulate the experimental investigation of propagation and interaction of light beams of arbitrary profiles (other than Gaussian) in photorefractive crystals.

References

1. Królikowski W., Luther-Davies B., Kivshar Y. *Opt. Electron. Rev.*, **9**, 287 (2001).
2. Królikowski W., Luther-Davies B., Denz C. *IEEE J. Quantum Electron.*, **39**, 3 (2003).
3. Khmelnitsky D., Matusevich V., Kiessling A., Kowarschik R., Ryzhova V.V., Shepelevich V.V., Zagorskiy A.E. *Ferroelectrics*, **390**, 18 (2009).
4. Shepelevich V.V., Golub A.A., Kowarschik R., Kiessling A., Matusevich V. *Kvantovaya Elektron.*, **35**, 352 (2005) [*Quantum Electron.*, **35**, 352 (2005)].
5. Shepelevich V.V., Golub A.A., Kowarschik R., Kiessling A., Matusevich V. *Appl. Phys. B*, **90**, 149 (2008).
6. Segev M., Valley G.C., Singh S.R., Carvalho M.I., Christodoulides D.N. *Opt. Lett.*, **17**, 64 (1995).
7. Singh S.R., Carvalho M.I., Christodoulides D.N. *Opt. Lett.*, **21**, 77 (1995).
8. Tiemann M., Halfmann T., Tschudi T. *Opt. Commun.*, **282**, 612 (2009).
9. Yajun L. *J. Modern Opt.*, **50**, 1957 (2003).
10. Dickey F.M., Holswade S.C. *Laser Beam Shaping Theory and Techniques* (New York: Marcel Dekker Inc., 2000).
11. Dorrer C., Zuegel J.D. *J. Opt. Soc. Am. B*, **24**, 1268 (2007).
12. Henderson B.G., Mansell J.D. *Proc. SPIE Int. Soc. Opt Eng.*, **7093**, 10 (2008).
13. Kukhtarev N.V., Markov V.B., Odoulov S.G., Soskin M.S., Vinetskii V.L. *Ferroelectrics*, **22**, 949 (1979).
14. Barkovskii L.M., Fedorov F.I. *Kristallografiya*, **10**, 174 (1965).
15. Królikowski W., Luther-Davies B., Denz C., Petter J., Weilnau C., Stepken A., Belić M. *Appl. Phys. B*, **68**, 975 (1999).
16. Motzek K., Stepken A., Kaiser F., Belić M.R., Ahles M., Weilnau C., Denz C. *Opt. Commun.*, **197**, 3161 (2001).
17. Yariv A., Yeh P. *Optical Waves in Crystals* (New York: Wiley, 1984).
18. Ducharme S., Feinberg J., Neurgaonkar R. *IEEE J. Quantum Electron.*, **23**, 2116 (1987).
19. Weber M.J. *Handbook of Optical Materials* (New York: CRC Press, 2003).
20. Garcia Quirino G.S., Irube Castillo M.D., Sanchez-Mondragon J.J., Stepanov S., Vysloukh V. *Opt. Commun.*, **123**, 597 (1996).
21. Roychoudhuri C., Kracklauer A.F., Creath K. *The Nature of Light: What is a Photon?* (*Optical Science and Engineering*) (Boca Raton: CRC Press/Taylor & Francis, 2008).
22. Cheng Y.-K., Lu Y.-H., Tien C.-H., Shieh H.-P. *J. Display Technol.*, **5**, 66 (2009).
23. Królikowski W., Denz C., Stepken A., Saffman M., Luther-Davies B. *Quantum Semiclass. Opt.*, **10**, 823 (1998).
24. Parent A., Morin M., Lavigne P. *Opt. Quantum Electron.*, **24**, S1071 (1992).